WOOD RESEARCH
64 (6): 2019
1101-1112

CHARACTERIZATION OF CEIBA PLYWOOD DELAMINATION IN MODE I USING AN ENERGETIC CRITERION

Anouar El Moustaphaoui, Abdelkarim Chouaf,
Khadija Kimakh, M'hamed Chergui
University of Hassan II
Casablanca, Morocco

(Received February 2019)

ABSTRACT

To characterize the delamination process of Ceiba plywood, an energy approach was used. This approach considers that crack propagation is a phenomenon of energy dissipation. The fundamental parameter of this approach is the energy release rate (G). To determine this parameter in pure mode I (G_I), a Double Cantilever Beam test (DCB) was deployed. The critical energy release rate in pure mode I (G_{IC}) is determined using four approaches, namely Beam Theory, Berry compliance law, Modified Beam Theory and the Compliance Calibration method. Then, a resistance curve of Ceiba plywood was determined according to each approach. Finally, a fracture surfaces analysis was discussed to understand the nature and types of fracture.

KEYWORDS: Plywood, delamination, DCB test, energy release rate, resistance curve, fracture surfaces.

INTRODUCTION

The arrival of derivatives and composites of wood, presenting characteristics more interesting than its natural form, gave a new industrial jump to this material (Claudel 2002). One of the best derivatives and composites of wood is the plywood panel. Plywood is a material used in many industries because it is a lightweight material and have high mechanical characteristics (Richard et al. 2003, Yasumura et al. 2006). Plywood is a very reliable product that has superior performance while maintaining comparatively high strength versus weight (Réh and Guoth 2016).

Plywood is a panel of thin wood sheets obtained by peeling. These sheets are called plies. This panel is distinguished by a superposition of crossed plies. The cohesion of the plies is ensured by gluing and hot pressing. In fact, the hot pressing could cause various macroscopic defects. Among these defects, there is delamination, micro-voids or impurities (Fougerousse

et al. 1982). The hot pressing is influenced by several parameters such as temperature, amount of glue, pressure, pressing time and moisture of the veneer. A false combination of these parameters could generate the delamination which will be the objective of our study.

In fact, delamination is a mechanism of failure which is characterized by a detachment or a decohesion between the plies of the laminate. The cause of delamination could be attributed, in large part, to the existence of interlaminar stresses. These interlaminar stresses develop from the discontinuity of the mechanical behavior between the individual plies (Avril 2009). The level of these stresses becomes very singular in the vicinity of the free edges, this phenomenon is known by the "free edge effect" (Vandellos 2011). At the level of these particular zones, the mode of opening (mode I) is the most critical delamination mode because it requires the least energy. The delamination is a predominant mode of failure in stratified structures subjected to mechanical loading, then the mastery of their initiation and their propagation is unavoidable. In fact, the predictions resulting from the numerical simulation of the behavior of a structure are insufficient to explain the reality without taking into account the law of delamination behavior. The determination of this law, above all, must be based on the analysis of experimental results obtained by the mechanical tests (Mathews and Swanson 2007).

MATERIAL AND METHODS

Material

To perform the DCB tests, the prismatic specimens of 9-ply plywood with the following dimensions (Fig. 1) were prepared.

Tab. 1: Dimensions of DCB specimens.

Length (w)	Width (b)	Thickness (h)
240 mm	80 mm	18.6 mm

During the manufacture of the specimens, the initial crack (a0) is produced by insertion of a thin teflon film with a thickness of 13 μm serving as an initiator for delamination. This pre-crack, necessary to initiate the delamination under stable conditions.

The glue used consists of the urea-formaldehyde (UF). The UF products are highly crosslinked, semi-crystalline thermosetting plastics. The UF resins are used for their high strength, rigidity, cost effectiveness, and fast cure.

Ceiba is a species widely used in the manufacture of plywood. It has interesting physical and mechanical properties for the manufacture of plywood. The moisture of the wood used to prepare the specimen is equal to 8%. The plies constituting the Ceiba plywood are 2 faces with a thickness of 0.8 mm, 3 cores with a thickness of 3 mm and 4 interiors with a thickness of 2 mm.

The hot pressing of plywood was consists in a first step in cold pre-pressing of the cross-ply composite panels at a pressure of 2 $kg \cdot cm^{-2}$. After pre-pressing, these panels are then introduced into a hot press so as to obtain sufficient polymerization of the glue film furthest from the heating plates. This hot pressing was ensured the physical and chemical bonding of various plies. The pressure, temperature and pressing time are determined by taking into account the type of adhesive, the thickness of the panel and the types of veneer used.

Determination of compliance and the critical energy release rate G_{IC}

To characterize this failure mode, the Double Cantilever Beam test (DCB) was deployed (Fig. 1a). This test consists of propagating a crack within a joint strained under tension and

measuring the resistance of this joint to the propagation of this crack. This test is applied to two lips of a specimen including an artificial crack.

The machine used to carry out the tests is a universal test machine type MTS 810 (MTS Systems Corporation) (Fig. 1b), which allows the conduction of controlled tensile tests. This machine records the variations of the load according to the imposed displacement. The imposed displacement records are provided by sensors installed on the machine. The loading velocity is equal to 2 mm·min^{-1}.

From this test, we can measure the tenacity of the interface G_{IC}, and draw the resistance curve, also called curve *R*. The first designates the resistance to the initiation of delamination, and the second describes the amount of energy necessary to propagate the initial crack (Lachaud 1997).

In this study, a series of DCB tests was carried out. From these tests, a typical curve of the load-displacement response (P-δ) will be presented. From these experimental results, the critical energy release rate (G_{IC}) can be determined by four approaches. Once these values are known, it will be possible to predict and anticipate the delamination of the plywood. Indeed, the G_{IC} is influenced not only by the accuracy of the stress and displacement measurements, but also by the accuracy of the measurements of the crack length and the variation in compliance with the crack length (Ducept et al. 1999).

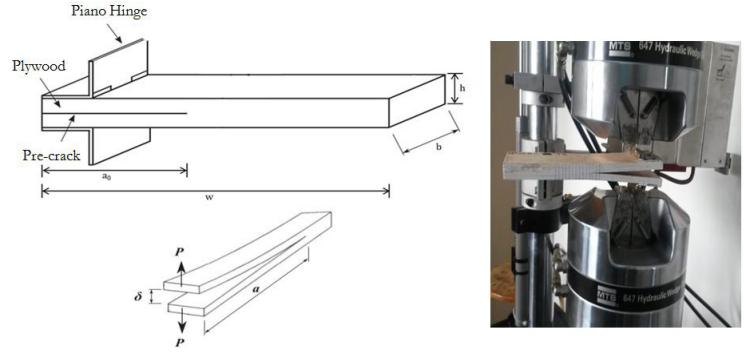

(a) *(b)*

Fig. 1: (a) DCB specimen and dimensions, (b) universal test machine type MTS 810.

To determine experimentally the compliance as well as the critical energy release rate G_{IC} relative to the structure studied, four different methods were deployed. The formalism of each of these methods is developed below:

Beam Theory Method (BT)

In order to evaluate the tenacity in pure mode I using DCB tests, Irwin-Kies formula resulting from the linear elastic mechanics of the rupture is applied (Irwin 1958):

$$G_{IC} = \frac{P_C^2}{2b}\frac{dC}{da} \qquad (\text{J·m}^{-2}) \qquad (1)$$

where P_C designates the critical load at the crack initiation, C the compliance of the specimen at the point of application of the load, b the width of the specimen and the initial crack length.

The classical beam theory, which neglects the shear effect, makes it possible to express compliance according to the crack length and the parameters of the material as follows:

$$C = \frac{2a^3}{3EJ} = \frac{\Delta\delta}{\Delta P} \qquad (\text{mm}\cdot\text{N}^{-1}) \tag{2}$$

where E is the longitudinal Young's modulus, δ the displacement between the two lips of the specimen and J the quadratic moment.

Taking account of Eqs. (2) and (3), the critical energy release rate can be written:

$$G_{IC} = \frac{3\delta_C P_C}{2ba} \qquad (\text{J}\cdot\text{m}^{-2}) \tag{3}$$

where δ_C corresponds to the displacement for which the critical load P_C is reached.

Compliance Calibration Method (CC)

The compliance law proposed by Berry is a power law. It can be written (Camanho 2002):

$$C = \alpha a_0^n \qquad (\text{mm}\cdot\text{N}^{-1}) \tag{4}$$

where α and n are parameters intrinsic to the material which are determined by the interpolation of the experimental curve C as a function of a_0. By applying this law of compliance, the formula Irwin-Kies makes it possible to obtain the critical energy release rate by:

$$G_{IC} = \frac{P_C^2}{2b}\alpha n a_0^{n-1} \qquad (\text{J}\cdot\text{m}^{-2}) \tag{5}$$

Modified Beam Theory (MBT)

The modified beam theory is a law of compliance, inspired by the beam theory that has been widely applied in the literature (Ducept et al. 1999):

$$C = A\, a_0^3 + B \qquad (\text{mm}\cdot\text{N}^{-1}) \tag{6}$$

where A and B are determined by a linear regression of the experimental curve of compliance C as a function of a_0^3. According to this formulation, the critical energy release rate can be expressed by:

$$G_{IC} = \frac{3P_C^2}{2b} A a_0^2 \qquad (\text{J}\cdot\text{m}^{-2}) \tag{7}$$

Compliance Calibration Method (CC)

It consists in drawing the logarithm of compliance, *log(C)*, as a function of the logarithm of the initial crack length $log(a_0)$. We determine the best linear approximation with the least squares method and we calculate the coefficient of the slope n.

Therefore, the critical energy release rate can be expressed by (O'brien 1998):

$$G_{IC} = \frac{n\,\delta_C P_C}{2ba} \qquad (\text{J}\cdot\text{m}^{-2}) \tag{8}$$

RESULTS AND DISCUSSION

Load-displacement curves

To determine the tenacity of Ceiba plywood, several cases of the ratio a_0/w were considered. To represent the results, Fig. 2 reports the most striking cases (a_0 / w = 0.37 - 0.42 - 0.47). For each crack length, a displacement load curve is presented.

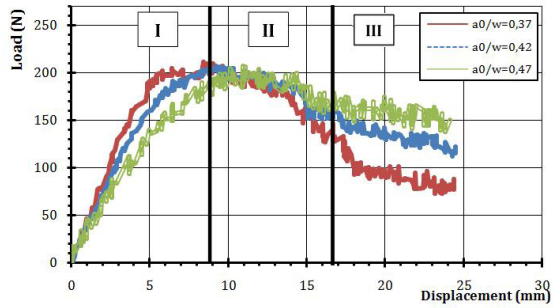

Fig. 2: Load-displacement curves for a_0 / w = 0.37; a_0 / w = 0.42 and a_0 / w = 0.47.

By analyzing the curves plotted in Fig. 2, three main phases of the behavior can be distinguished during the test:

In the first part (step I), the load increases linearly with the displacement imposed until the delamination starts. Then, at the beginning of the propagation of the crack, we observed an increase in the load followed by a stage where the charge remains almost stable (step II). Finally, the propagation of delamination results in a decrease in stress as a function of the evolution of the crack (step III).

In general, the relatively smooth curves represent the stable propagation of the crack, while the drop in load indicates a propagation of the unstable crack. During the tests, the evolution of the crack remained relatively stable.

The local disturbance of the load-displacement curve is due to the bridging of the fibers. The increase in load is associated with the creation of a fiber bridge, while the fall of the load indicates the breaking of the bridge. During the tests, the growth of the crack remained relatively stable. The bridging of the fibers formed at the bottom of the crack seems important.

The critical energy release rate G_{IC}

From the DCB tests, the determination of the value of G_{IC} rests on two pillars:

- The first concerns the definition of initiation point of the crack on the load-displacement curve. According to the standards, the starting point can be the point marking the end of the linearity, or the point representing a 5% decrease in the initial steering coefficient.
- The second is the choice of a model of the law of compliance required in the use of the Irwin-Kies formula.

In this study, the point marking the end of the linearity of the load-displacement curve is indeed the beginning of the propagation of the crack.

To determine experimental compliance, the load-displacement curve has been plotted for several initial crack length a_0. Then, the load equation was determined as a function of the displacement δ in the linear part. The experimental compliance was calculated using Eq. 2.

In order to compare the results obtained from the four approaches, the compliance of each specimen must be determined. Then, it is necessary to perform interpolations according to the Berry compliance Law (Fig. 3), the linear law in a_0^3 resulting from the modified beam theory (Fig. 4) and the Compliance Calibration Method (Fig. 5).

The tests performed can be considered as stable because there is no abrupt change in the load during loading imposed displacement. There is no unstable crack propagation either.

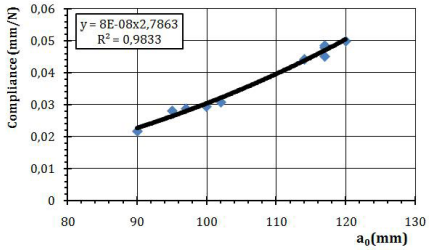

Fig. 3: Plot of the compliance vs. the initial crack length a_0.

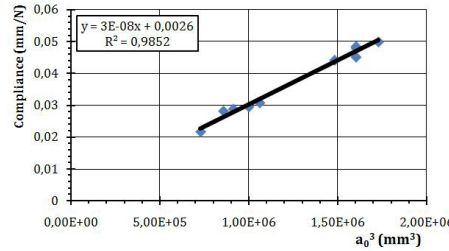

Fig. 4: Plot of the compliance vs. the cubic of initial crack length a_0^3.

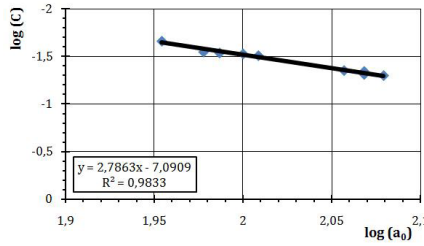

Fig. 5: Plot of the logarithm of the compliance log(C) vs. the logarithm of the initial crack length log(a_0).

After determining the laws of experimental complacency according to the four experimental approaches, the equations of the trend curves were used to calculate the critical energy release rate G_{IC}.

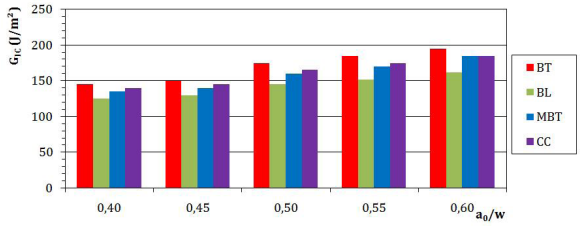

Fig. 6: G_{IC} according to the four approaches.

After determining the laws of experimental compliance according to the three experimental approaches, the equations of the trend curves were exploited to calculate the critical energy release rate G_{IC} using Eqs. 3, 5, 7 and 8. The regression coefficients of the trend curves are all close to 1. To better compare the critical energy release rate G_{IC} from the four approaches, they reported them together in Fig. 6.

According to the results obtained, we can observe that each method of experimental compliance is in good agreement with the analytical method of beam theory.

For an initial crack length a_0/w = 0.50, the variation of the three experimental approaches with respect to the beam theory approach was determined. The critical energy release rate G_{IC} calculated according to the four approaches is mentioned in Tab. 2.

Tab. 2: Comparison between the G_{IC} resulting from the experimental approaches and that of beam theory for a_0/w=0,50.

	Beams theory	Berry's Law	Modified Beam Theory	Compliance Calibration
G_{IC} (J·m^{-2})	175	145	160	165
Standard deviation (J·m^{-2})		30	15	10
Coefficient of variation (%)		17.14	8.57	5.71

From these results, it is clear that the beams theory gives the highest results; on the other hand the Berry's law gives the lowest results. The deviations of the experimental approaches do not exceed 17% compared to the beam theory.

Indeed, the BT method does not take into account the rotation of the microcracks in the delaminated zone. This causes an overestimation of G_{IC} values. Therefore, it is recommended to use the experimental approaches which take into account the rotation of the microcracks and the bridging of the fibers in the delaminated zone.

Resistance curve

Due to the variation of the energy release rate as a function of the crack length, the delamination study cannot be treated correctly only by a single G_{IC} value, but the behavior of delamination propagation must be studied, and this is possible thanks to the resistance curve.

To describe the evolution of the resistance to delamination as a function of the increase of the crack after the starting point of the delamination, a resistance curve has been plotted. This curve is based on the determination of the energy release rate G_I.

To do this, G_I was determined according to the four approaches from the results of the experimental compliance curves C as a function of initial crack length a_0 previously determined. Then the Eqs. 3, 5, 7 and 8 were used by replacing the critical load P_c by the load associated with the crack length a.

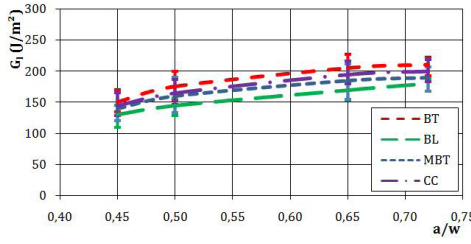

Fig. 7: R-curve of the four approaches (a_0/w = 0.45).

To determine the crack length a, a camcorder was used to track the evolution of the crack propagation. Whenever the crack reaches a graduation on the edge of the specimen, the associated load and displacement are recorded.

In Fig. 7, the average values of the energy release rate G_I of several specimens which have the same initial crack length a_0 (a_0/w = 0.45) have been shown. These average values of the energy release rate are framed by more than at least one standard deviation.

According to the results obtained, we can notice than the delamination resistance represents the same behavior for all analytical and experimental approaches. The energy release rate is proportional to the crack length. The increasing evolution of this R-curve involves the influence of fiber bridging.

To better compare the results obtained from the delamination resistance of Ceiba plywood with other composites, we have grouped in Tab. 3 the energy release rate of the carbon/epoxy (Prombut et al. 2006) and glass/epoxy (Alsaadi and Erkliğ 2017).

Tab. 3: Comparison between the G_{IC} of Ceiba plywood, carbon/epoxy and glass/epoxy.

	Ceiba Plywood	**Carbon/epoxy (T700/M21)**	**Glass/epoxy (Perlite)**
G_{IC} (J·m^{-2})	125 - 195	501 - 579	550 - 700

It is quite normal that the delamination resistance of Ceiba plywood is lower than other composites based on carbon/epoxy and glass/epoxy.

To better examine this fracture behavior which passes through the stages of initiation and propagation of the crack, a fracture surfaces analysis was discussed.

Analysis of fracture surfaces

The analysis and interpretation of fracture surfaces of broken DCB specimens is essential to understand the nature of their fracture. Indeed, the examination of the fracture surfaces makes it possible to detect, after rupture, the mechanism of failure and the type of cracking produced. Generally, the surfaces of a broken specimen have several zones: a zone of initiation and a zone of propagation of crack (first stable then rapid evolution).

In this analysis, macroscopic observations seem sufficient to interpret fracture surfaces.

After examining all fracture surfaces, three types of failure have been distinguished:

- Cohesive failure that takes place when the break occurs within the adhesive layer (Fig. 8a).
- An adhesive failure that corresponds to a break at the interface between the substrate and the adhesive (Fig. 8b).
- A failure of the substrate which corresponds to the rupture within the substrate (Fig. 8c).

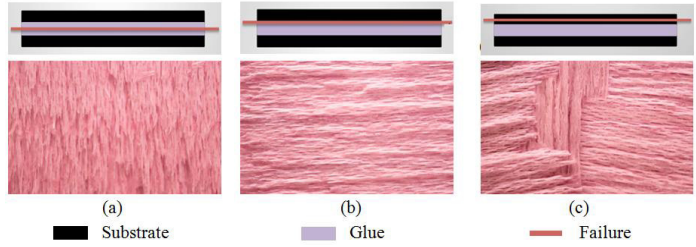

Fig. 8: Fracture surfaces: (a) Cohesive failure, (b) Adhesive failure, (c) failure of the substrate.

Fig. 8a illustrates the propagation of delamination in the joint of the glue. This delamination starts with microfissurations of the resin. These microfissurations develop to a critical state where failure of the resin inside the fold occurs, which causes the fall of the load (Fig. 3). In this case, the resistance of the adhesive layer to the loading is assumed to be lower than the adhesive loads between adhesive and substrates.

Fig. 8b illustrates the propagation of delamination out of the joint of the glue. The good adhesion of the resin causes to breaking of the fibers, and this is followed by a fall of the load

(Fig. 9). However, it should be noted that this failure is never purely adhesive, as the observations show that there is always a residue of adhesive on the substrate after such a break.

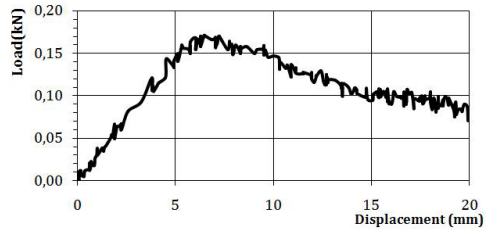

Fig. 9: Load-displacement curve in the case of adhesive failure.

Fig. 8c illustrates a failure of the substrate. In this case, the tenacity of the adhesive layer does not intervene, but rather the rigidity of the substrate which takes part, according to the applied stress. The breaking of the substrate causes a brutal fall of the load, followed by a step where the charge remains almost stable (Fig. 10).

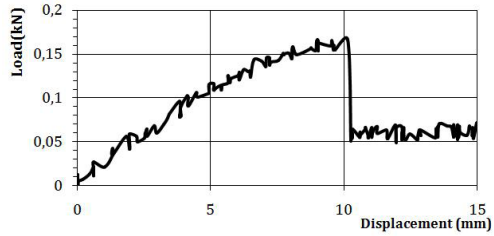

Fig. 10: Load-displacement curve in the case of failure of the substrate.

Indeed, the combination of delamination and intralaminar damage can lead to early breakage of the laminates. The coupling between transverse damage and delamination has also been highlighted by many authors in the case of the impact on laminates (Renault 1994, Guinard et al. 2002). This is why the study of the influence of intralaminar damage on delamination represents an important current issue to fully describe the failure of laminates under certain stresses.

CONCLUSIONS

The development of the use of plywood panel in new structures is through the improvement of its behavior by seeking to understand and master the complex phenomenon of delamination of this material.

In this study, the characterization of delamination of Ceiba plywood panels was discussed. This panel is distinguished by its good resistance to delamination. To characterize pure mode I, the most used configuration is the DCB test. The approaches deployed are the beam theory method, Berry compliance law, modified beam theory and compliance calibration method. Indeed, it is recommended to use experimental approaches that take into account physical phenomena such as shear deflection and fiber bridging. In addition, they have the advantage over finite element methods of not being dependent on the identification of the mechanical properties

of the material especially for a complex material such as wood. Then, the resistance curve of the studied structure was established. From these tests, the critical values of the tenacity of pure mode I material were determined according to each crack length. For a value of a_0/w = 0.40, the G_{IC} is of the order of 135 J·m^{-2}, whereas for a value of a_0/w = 0.60 the G_{IC} is of the order of 180 J·m^{-2}. These are the values that will allow us to predict and anticipate the delamination of Ceiba plywood.

The analysis of fracture surfaces is excessively rich in terms of the type of damage. There are generally three zones of damage respectively corresponding to the initiation phase, stable propagation and instantaneous final rupture. Experimentally, it is often difficult to know precisely the mechanisms of crack initiation. According to our experiments, the propagation of the delamination is done in two ways, a delamination which starts with microfissurations of the resin, these microfissurations develop to a critical state where failure of the resin inside the fold occurs, and delamination out of the joint of the glue. In the latter case, the good adhesion of the resin causes the breaking of the fibers followed by a fall of the load.

REFERENCES

1. Alsaadi, M., Erkliğ, A., 2018: Effect of perlite particle contents on delamination toughness of S-glass fiber reinforced epoxy matrix composites. Composites Part B 141: 182-190.
2. Avril, C., 2009: Experimental and numerical study of interlaminar resistance in mode I of thermoplastics with woven reinforcement. Philippe OLIVIER et Jacques LAMON. JNC 16, Toulouse, France.
3. Camanho, P.P, Dávila, C.G., 2002: Mixed-mode decohesion finite elements for simulation of delamination in composite materials. NASA/TM-2002-211737, 37pp.
4. Claudel J.B., 2002: Characterization of the mechanical behavior of plywood panels under flexural stress and bending-compression. PhD Thesis. Université de Metz, France.
5. Ducept, F., Gamby, D., Davies, P., 1999: A mixed-mode failure criterion derived from tests on symmetric and asymmetric specimens. Compos Science and Technology 59: 609-619.
6. Fougerousse, M., Barray, R., Deon, G., 1982: Resistance of plywood panels to rot: first tests on the influence of ply thickness. Revue Bois et Forêt des Tropiques 19: 61-71.
7. Guinard, S., Allix, O., Guédra-Degeorges, D., Vinet, A., 2002: A 3D damage analysis of low-velocity impacts on laminated composites. Composites Science and Technology 62: 585-589.
8. Irwin, G.R., 1958: Fracture in encyclopedia of physics, edited by S. Flucge, Vol. VI. Fracture, Springer Verlag, Pp 551-590.
9. Lachaud, F., 1997: Delamination of composite materials with carbon fibers and organic matrices: Numerical and experimental study, followed by acoustic emission. PhD Thesis, Université Paul Sabatier, Toulouse, France.
10. Mathews, M.J., Swanson, S.R., 2007: Characterization of the interlaminar fracture toughness of a laminated carbon/epoxy composite. Composites Science and Technology 67: 1489-1498.
11. O'brien, T.K., 1998: Interlaminar fracture toughness: the long and winding road to standardization. Composites Part B Eng 29: 57-62.
12. Prombut, P., Michel, L., Lachaud, F., Barrau, J.J., 2006: Delamination of multidirectional composite laminates at 0^°/θ^°ply interfaces. Engineering Fracture Mechanics 73: 2427-2442.

13. Renault, M., 1994: Compression after impact of a stratified plate: experimental study and modeling associated finite elements. Thèse de doctorat, Ecole Centrale de Nantes, France.
14. Richard, N., Yasumura, M., Davenne, L., 2003: Prediction of seismic behaviour of wood framed shear walls with openings by pseudodynamic test and FE model. The Japan Wood Research 49: 145-151.
15. Réh, R., Guoth, M., 2016: Thermoplastic plywood and it's drawback when moderately heated. Wood Research 61(6): 895-902.
16. Vandellos, T., 2011: Towards a model of cohesive zones adapted to the study of delamination in stratiated composites. 10th national colloquy on calculating structures, Giens, France.
17. Yasumura, M., Kamada, T., Imura, Y., Uesugi, M., Daudeville, L., 2006: Pseudodynamic tests and earthquake response analysis of timber structures II: two-level conventional wooden struc-tures with plywood sheathed shear walls. Journal of Wood Science 52: 69-74.
18. Yasumura, M., Yasui, S., 2006: Pseudodynamic tests and earthquake response analysis of timber structures I: plywood sheathed conventional wooden walls with shear openings. Journal of Wood Science 52: 63-68.

Anouar El Moustaphaoui*, Abdelkarim Chouaf
Khadija Kimakh, M'hamed Chergui
University of Hassan Ii
National Superior School of Electricity And Mechanics
El Jadida Road, Km 7
Pb: 8118 Oasis – Casablanca
Maroc
*Corresponding author: anouar.most@gmail.com